Eur. Phys. J. D **11**, 115–122 (2000)

THE EUROPEAN PHYSICAL JOURNAL D

EDP Sciences

Second harmonic generation in deposited clusters

C. Kohl[1,2], E. Suraud[3,a], and P.-G. Reinhard[4]

[1] Physics Department, University of Washington, Seattle, USA
[2] GE CompuNet, Hörselbergstrasse 7, 81677 München, Germany
[3] Laboratoire de Physique Quantique, Université Paul Sabatier, 118 route de Narbonne, 31062 Toulouse Cedex, France
[4] Institut für Theoretische Physik, Universität Erlangen, Staudtstrasse 7, 91058 Erlangen, Germany

Received 22 October 1999 and Received in final form 14 December 1999

Abstract. We analyse theoretically the generation of second and higher harmonics for sodium clusters deposited on an insulating surface. To this end, we use the time-dependent local-density approximation solved on a three-dimensional grid. We explore the impact of the various laser parameters (intensity, frequency, polarisation) on the efficiency of second harmonic generation. The success sensitively depends on a proper tuning of these parameters. We find optimum conditions for which the laser frequency is half the resonance frequency of the system, if the polarisation is directed orthogonal to the surface of the substrate, and if the intensity is large but safely below the critical value for destruction of the electron cloud.

PACS. 36.40.Vz Optical properties of clusters – 42.65.Ky Harmonic generation, frequency conversion

1 Introduction

Optical response is a key tool for the study of metal clusters. It has intensively been exploited over the past decades to analyse cluster structure and dynamics, for reviews and monographs see [1–4]. The bulk of these former investigations has been concerned with the regime of linear response. More recently, the technological developments have allowed to produce highly excited electronic states, *e.g.* after excitation by highly charged ionic projectiles [5] or by irradiation with intense lasers [6]. This regime of strong excitations opens worlds of new phenomena. Strong ionisation renders the clusters Coulomb-unstable and leads to fission or fragmentation [7,8]. A bit more moderate external fields allow to resolve the detailed emission patterns of photoelectrons [9], or the extraction of the plasmon width from laser irradiation of deposited clusters [10]. The theoretical tools for an efficient description of such situations can nevertheless still be found in the realm of effective mean-field theories founded on the Density Functional Theory (TDDFT) [11], pioneered by the work of [12]. The practical implementation is then done by means of the fully fledged time-dependent local-density approximation (TDLDA) solved, without any linearization, directly in the time domain [13,14]. It is the simplest approach staying at the level of a local and adiabatic TDDFT, and this is the line we will pursue here.

Moderate electronic excitations are a fascinating field of investigation for cluster science because they mix up non linear effects to sizable traces of structural properties. In the case of metal clusters a typical example for this intermediate regime is the search for harmonic generation (Second Harmonic Generation, SHG) following laser irradiation. In the strictly linear regime, the cluster's response to an irradiation takes place exclusively at the excitation frequency. With increasing laser intensity, an-harmonic effects quickly show up and lead to the appearance of side peaks at integer multiples of the excitation frequency. The strength of these peaks decreases with multiplicity and the dominant process is usually frequency doubling, called SHG. Beyond its mere interest as such, SHG in clusters has been used for example to trace the impact of intermediate excitations, in terms of Mie plasmon decay [10]. There are also applications to frequency doubling of laser beams, once particularly suited crystals are used. First and elementary theoretical considerations on SHG for metal clusters have been presented in [15]. It is the aim of this paper to investigate SHG theoretically using the more detailed TDLDA as a tool.

Most experiments devoted to SHG or SHG applications have been performed with deposited metal clusters [10,16]. A technical reason is that this allows a higher density of clusters which then helps to gather a sufficiently strong signal from the second harmonics. A physical reason is that SHG requires broken reflection symmetry because only this allows that SHG transforms a squared dipole excitation into one dipole signal, *i.e.* $\hat{D}^2 \longrightarrow \hat{D}$. That transition cannot be mediated by a reflection symmetric system because parity is then conserved, but $\hat{D}$ has negative parity while $\hat{D}^2$ has positive parity. Free clusters are too symmetric, which can be seen from the fact that their shapes contain usually only very small octupole (or higher odd multipole) moments. Thus they produce only

[a] e-mail: suraud@irsamc2.ups-tlse.fr

faint SHG, and even this may be completely wiped out by destructive interference of the signals from the stochastically oriented clusters [17]. At a quantitative level, one has to take into account furthermore the fact that the response of a free cluster comes usually very close to harmonic vibrations, which adds a general suppression of higher harmonics. A solid surface, however, represents a strong symmetry breaking, first, because it divides the space into two distinct regions, and second, because the strong surface interaction induces additional deformation of the cluster. The breaking of reflection symmetry does also help to spoil the "harmonicity" of the free response [18]. Clusters attached to a surface are thus the ideal setup for producing SHG. We will consider the case of metal clusters attached to an insulating surface, in particular we take here as test case a Na_8 cluster on a NaCl substrate. This test case is by far smaller than the clusters used in the actual measurements which contain several thousands of ions [16]. This is, of course, a tribute to the technical limitations of today's TDLDA computations. But we expect that the basic trends can be sufficiently well explored with this manageable test case.

The paper is organized as follows. Section 2 is devoted to a short survey of the theoretical model used to describe deposited clusters and the tools of analysis of SHG. In Section 3 we discuss typical results and explore the impact of the laser parameters on the quality of the SHG response. Some conclusions and perspectives are finally presented in Section 4.

2 The framework

2.1 Description of the deposited clusters

In this paper we use the methods developed in [19] to describe the deposited cluster and its electronic dynamics. We recall here briefly the essential ingredients. The treatment is much simplified due to the fact that the NaCl substrate remains essentially inert as shown by detailed *ab initio* calculations [20]. The description can then be reduced to account only for the valence electrons and the ions of the cluster itself. This was extensively investigated in [19,21] and it was shown that the effect of the NaCl substrate can indeed be incorporated into an appropriate interface potential.

The valence electrons of the Na atoms of the cluster are described by TDLDA. The single electron wavefunctions $\psi_\alpha(\mathbf{r},t)$ thus follow the time-dependent Kohn-Sham equations [22] which are explicitly solved in real time, by projection onto an equidistant numerical grid [23]. The Kohn-Sham potential acting on electrons is thus composed as

$$v_{\rm KS}(\mathbf{r},t) = \int {\rm d}^3r' \, \frac{\rho(\mathbf{r}',t)}{|\mathbf{r}-\mathbf{r}'|} + v_{\rm xc}(\mathbf{r},t) + v_{\rm psp}(\mathbf{r},t) + v_{\rm surf}(\mathbf{r},t) + e\hat{\mathbf{D}}\cdot\mathbf{E}_{\rm laser}(\mathbf{r},t) \quad (1)$$

where the first two terms describe the interacting electron cloud of density $\rho(\mathbf{r},t)$ and the other three terms the external influences. The $v_{\rm psp}$ term takes into account the electron-(cluster)-ion interactions *via* pseudo-potentials. The $v_{\rm surf}$ contribution mediates the interaction with the substrate. And the last term describes the laser field, see equation (2). Actually, we work here with the local spin-density approximation (TD-LSDA) and for $v_{\rm xc}$ we use the spin-dependent parameterization of Gunnarsson and Lundqvist [24]. The pseudopotential for $v_{\rm psp}$ can be chosen as local [25]. We use here the parameterization of [19]. Finally, the interaction amongst the ions of the cluster is the simple point-like Coulomb interaction. It does not play a role in the present investigations because the ions are considered to be frozen during laser excitation.

A few words are in place about the $v_{\rm surf}$ term. Electrons and ions are coupled to the substrate by an interface potential. Indeed the *ab initio* calculations of [20] have shown that the substrate is only very little affected by the attached cluster. There is a negligible charge transfer for the adsorbed monomer, no signs for the formation of a chemical bond, no overlap with substrate states and consequently no hybridization. A simple ansatz hence consists in mapping the *ab initio* results into an interface potential with a few adjustable parameters. This potential incorporates the Coulomb forces of the substrate as well as the surface polarisation due to the ad-atoms. It is adjusted to the exact results [20] for one ad-atom and for the Na_8 cluster on the surface. The emerging fit then reproduces nicely all available other combinations of small Na clusters on NaCl [19,21]. We thus continue along this line and use the interface potential of [19] with the same set of parameters. Contributions to the SHG from the substrate are hence neglected. This is probably a fair approximation because the pure surface without clusters has little response at all in the considered frequency range.

2.2 Spectral analysis of SHG

Our deposited clusters are irradiated by laser fields which we treat in the dipole approximation. We use linearly polarised lasers. The cluster is thus subject to an external, time dependent, electric field

$$\mathbf{E}_{\rm laser}(\mathbf{r},t) = E_0 f(t) \sin(\omega_{\rm laser} t)\mathbf{u} \quad (2)$$
$$f(t) = \cos^2\left(\frac{t-T_{\rm pulse}}{T_{\rm pulse}}\frac{\pi}{2}\right)$$

where $\mathbf{u}$ labels the polarisation vector and $\omega_{\rm laser}$ the frequency of the laser. The intensity I of the laser fixes the amplitude E_0 of the exciting field ($I \propto E_0^2$) and the pulse profile $f(t)$ is here a $\cos^2$ pulse with FWHM = $T_{\rm pulse}$ = 50 fs. The electronic response is predominantly concentrated in the dipole mode, which can be accessed through the dipole moment of electrons

$$\mathbf{D}(t) = \langle e\mathbf{r}\rangle = e\int \rho(\mathbf{r})\mathbf{r}\,{\rm d}\mathbf{r}, \quad (3)$$

where $\mathbf{r}$ is measured with respect to the centre-of-mass of the cluster's ions. In the strictly linear domain, the dipole

response of an excited cluster is harmonic and proportional to the exciting laser field $\mathbf{E}_{\text{laser}}$. The proportionality constant is just the coefficient (generally a tensor in non-isotropic systems) of linear dynamical polarisability α_1, *i.e.* $\mathbf{D}(t) = \Re\left\{\alpha_1(\omega_{\text{laser}})E_0 \exp\left(-\mathrm{i}\omega_{\text{laser}}t\right)\right\}\mathbf{u}$. But non linear effects couple to sidebands of multiple frequencies and thus higher harmonics $\propto \exp\left(-\mathrm{i}n\omega_{\text{laser}}t\right)$ appear in the dipole signal. The first sideband to be considered lies at double frequency and is known as second harmonic generation (SHG).

Practically, the analysis of the optical response, and in particular of the SHG signal, is performed from real time dynamics. We let the system evolve for twice the laser FWHM (namely 100 fs), and record in time the dipole moment. A Fourier transform of $\mathbf{D}(t)$ into the frequency domain yields $\tilde{\mathbf{D}}(\omega)$, from which one can read off the dipole strength function in each direction as $S_i(\omega) = \Re\{\tilde{D}_i(\omega)\}$ and the power spectrum as $\mathcal{P}_i(\omega) = |\tilde{D}_i(\omega)|^2$ $(i \in \{x, y, z\})$. The strength function is directly related to the photo-absorption cross-section [26] and is well suited to the domain of linear response. The power spectrum is better adapted to analyse nonlinear effects, growth of dissipation and transition to spectral chaos [27]. For details on this kind of spectral analysis we refer the reader to [27]. Because by nature SHG is a non linear effect, we focus our present analysis on the power spectrum.

2.3 On the choice of laser parameters

The laser pulse equation (2) has several free parameters, frequency ω_{laser}, intensity $I \propto E_0^2$, pulse profile and length T_{pulse}, and polarisation $\mathbf{u}$. They all have their impact on SHG, which we will briefly discuss here in terms of general arguments. The practical results in the next section will then take up each dependence step by step as outlined here.

We have chosen here a $\cos^2$ profile for the laser pulse. This is good approximation to a Gaussian pulse and as such has a high spectral selectivity. Additionally, it switches off precisely at start and end ($t = 2T_{\text{pulse}}$) which makes it very efficient for numerical simulations. The pulse length is chosen rather short with $T_{\text{pulse}} = 50\,\text{fs}$, similar to experiments [16]. There are two reasons for it. First, one needs sufficient intensities to study non-linear effects and these are usually achieved by fs laser. Second, such short analysing times allow to keep the ions frozen. For longer pulses, ionic dynamics starts to mix with the laser excitation and would make the picture much more complicated.

The laser frequency ω_{laser} plays, of course, a key role. Former studies of irradiation of clusters by short intense laser pulses have demonstrated the importance of resonance with the Mie plasmon frequency ω_{plasmon}, *e.g.* effects on ionisation [28] or field amplification [29]. The same will continue to hold for SHG [10,16,30,31]. Preliminary theoretical investigations of this question have been presented in [32]. It was shown there that SHG is particularly pronounced when ω_{plasmon} is involved in the entrance or exit channel. A simple analytical estimate in a perturbed harmonic oscillator model suggests that SHG is particularly efficient if $\omega_{\text{laser}} = \omega_{\text{plasmon}}$ or if $2\omega_{\text{laser}} = \omega_{\text{plasmon}}$. The latter case corresponds to the so-called SHG "into resonance" as the laser is tuned so that the second harmonics exactly matches the plasmon resonance. It is the advantageous choice because this allows to work with a lower laser frequency which, in turn, reduces unwanted perturbations by electron emission. We will discuss in the following results for both choices and one further case completely out of resonance.

Table 1. Geometrical characteristics of Na_8 deposited on NaCl for 2D ground state and 3D isomer. The first two columns show the dimensionless multipole moments of the ionic distribution as defined in equation (4). The last three columns show the mean plasmon frequencies along the three principal cluster axes. Note that in the case of the 3D isomer only the dominant peak of the strongly Landau fragmented plasmons have been indicated.

	β_{20}	β_{30}	ω_x (eV)	ω_y (eV)	ω_z (eV)
2D ground state	0.86	0	1.7	2.4	3.54
3D isomer	0.07	0.24	2.65	2.65	2.65

The next crucial parameter is the laser intensity $I \propto E_0^2$. Indeed, SHG is a non-linear effect and requires sufficient intensity to produce a reasonable signal. On the other hand, very large intensities will perturb the system too much and thus destroy the electron response which we need for SHG. We thus expect that there is a window of most favourable laser intensities for SHG.

Finally, the choice of polarisation should also be investigated. Mind that we are considering deposited clusters in which there is a strong symmetry breaking through the surface. One can thus easily imagine that the direction perpendicular to the surface will not provide the same SHG as the directions along the surface. This actually also raises the question of cross talks between the various directions. In the most general case, one has to assume that the SHG response is a third order tensor. In practice, we find that cross talk is usually small and that most of the response is concentrated along the polarisation axis of the laser. For simplicity, we have thus restricted our investigations here to the on diagonal terms of the SHG tensor.

3 Results

3.1 Na_8 deposited on NaCl

Our test case is Na_8 deposited on the insulating NaCl surface. Two configurations will be considered. They are illustrated in Figure 1. The strong attractive interface interaction tries to pull all ions close to the surface, and thus the ground state has a planar monolayer 2D structure, see left part of Figure 1. As can be seen from Table 1, this 2D ground state configuration is strongly deformed and

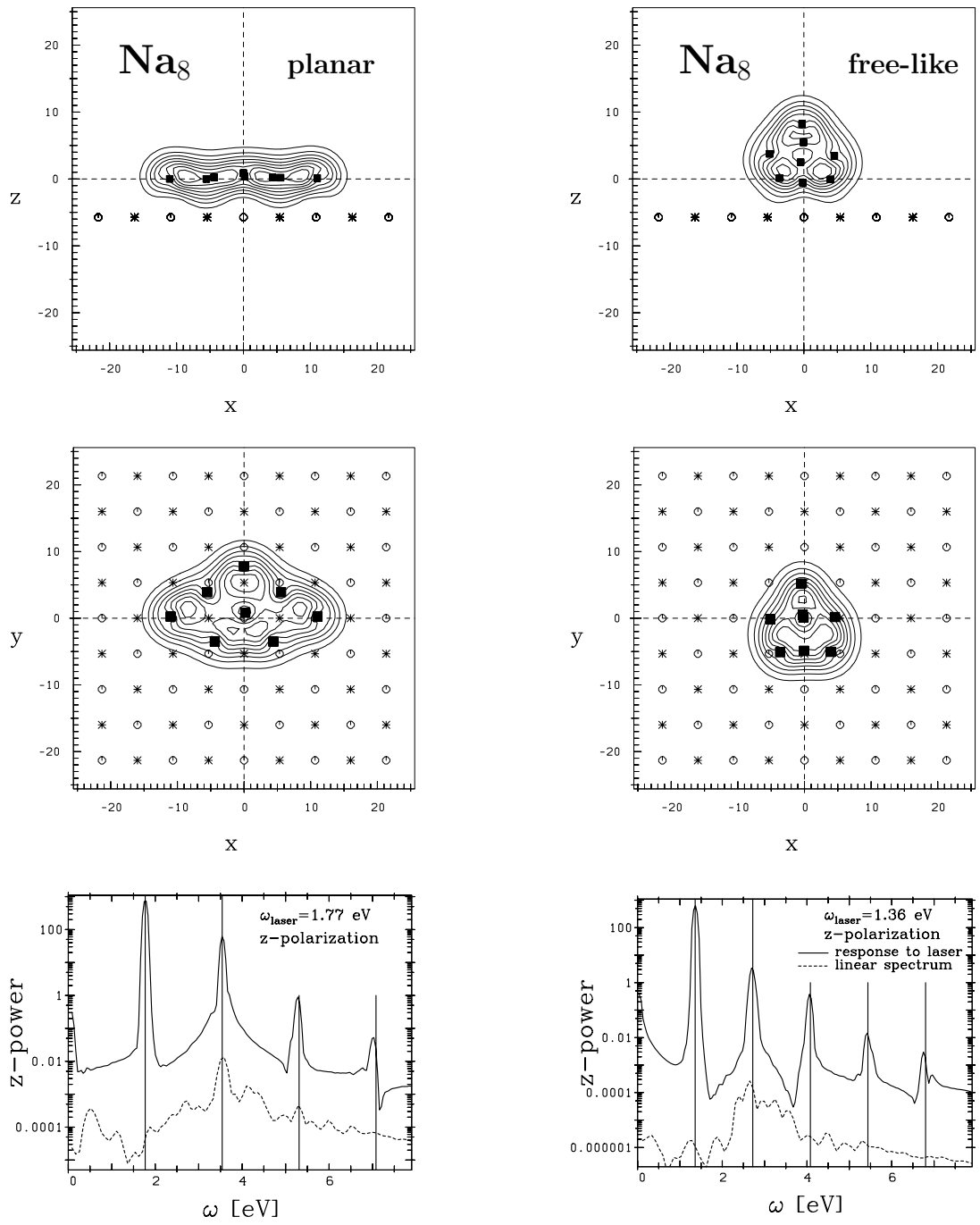

Fig. 1. Key features of 2D ground state (left column) and 3D isomer (right column) of deposited Na_8 on NaCl clusters. The two upper panels display iso-density contour plots of electrons. The upper panel shows a cut through the surface and the middle panel the distribution over the surface. The ions within the clusters are indicated by full squares, the Na ions of the substrate by open circles, and the Cl ions by stars. The bottom panels show spectral properties. The dotted lines represent the spectrum of (linear) dipole response along the z-axis and the full line is the spectrum of the response to a laser signal with frequency as indicated and polarised along z-axis. Note that the laser frequencies have been chosen so that the second harmonics coincides with the dominant Mie resonance.

triaxial. The planar structure nevertheless yields negligible octupole moment. But the interface interaction produces enough asymmetry for SHG. The Na_8 cluster has a magic electron number (remind that free Na_8 is close to spherical). This "magicity" is so strong that it can resist the flattening power of the interface and produces a quasi spherical 3D isomer which is only little higher in energy (0.05 eV) than the 2D ground state. This 3D isomer has virtually no quadrupole deformation but acquires a strong octupole moment with its typical pear shape, see right part of Figure 1. Complementing numbers are given in Table 1. Note that the global deformation of the clusters are expressed in terms of the dimensionless spherical quadrupole and octupole moments

$$\beta_{20} = \frac{4\pi}{5N}\frac{\langle r^2 Y_{20}\rangle}{\langle r^2\rangle}, \quad \beta_{30} = \frac{4\pi}{7N}\frac{\langle r^3 Y_{30}\rangle}{\langle r^3\rangle}\,. \tag{4}$$

As is well known, deformed clusters exhibit different spectra along different directions for simple geometric reasons [1]. The present test cases have naturally three principal axes: the normal (z) axis to the interface, and the x- and y-axes, which follow the two crystal orientations, parallel to the surface (see middle panels) [19]. Summarizing the results of [19], we report in Table 1 the mean plasmon frequencies along these principal axes for both the 2D and 3D clusters. The 2D ground state exhibits three well separated frequencies corresponding to the fact that the three principal axes have very different lengths (the longer the axis, the smaller the frequency). In turn the mean frequencies of the "almost spherical" 3D isomer are very close together. It is to be noted, however, that this case is distinguished by a strong Landau fragmentation of the plasmon resonances [19] which is due to the large octupole deformation [18]. Moreover, the observed mean frequency of the 3D isomer is red shifted as compared to the Mie plasma frequency. This is an effect which appears already for free clusters and it can be related to surface effects, particularly to the electronic spill-out [2]. Table 1 and subsequent discussion are thus complemented by showing the dipole power spectra for the eigenmodes along the z-axis in the lowest panels of Figure 1. One sees clearly the well developed plasmon resonance and its fragmentation in the case of the 3D cluster.

Finally, the bottom panels of Figure 1 provide a first demonstration of SHG. The full lines show the dipole power spectra as results of laser excitation with the laser parameters as indicated. The laser has been polarised, in both cases, perpendicularly to the surface (*i.e.* in z-direction) and the spectral analysis is performed along the same z-axis. The laser frequencies have been tuned to the most favourable case, namely such that $2\omega_{\rm laser}$ coincides with the plasmon peak. And quite expectedly, we see in both cases well developed SHG and higher harmonics (multiple laser frequencies are indicated by vertical lines). The first peak corresponds to the excitation frequency $\omega_{\rm laser}$ itself. The SHG signal is the second peak (at $2\omega_{\rm laser}$) and the higher harmonics follow. Note the very good ratio of peak over background noise (10^5 for the direct response, still about 10^4 for SHG). This proves that we have indeed successfully tuned the proper conditions for SHG with the choice $2\omega_{\rm laser} = \omega_{\rm plasmon}$.

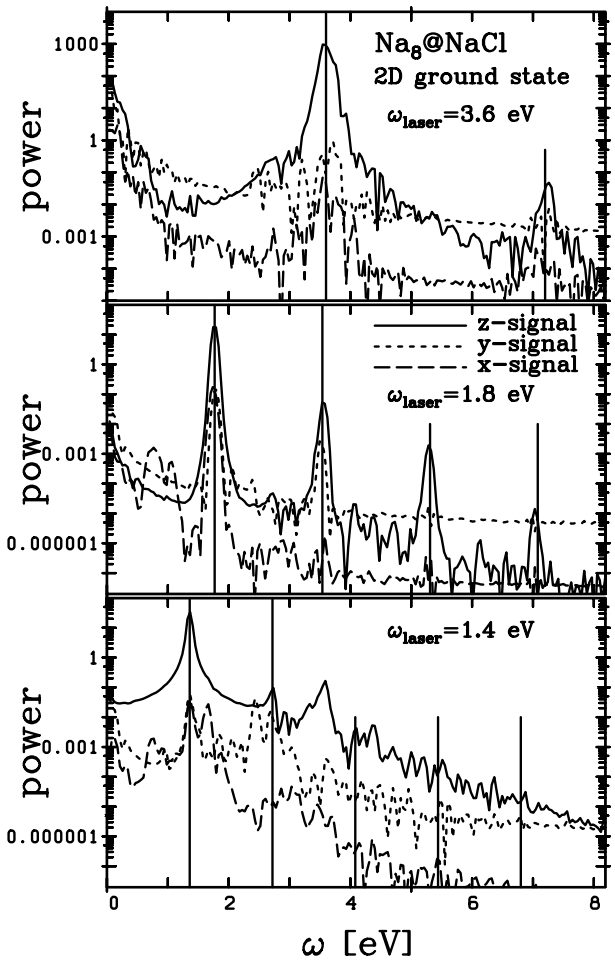

Fig. 2. Influence of laser frequency on SHG response in the case of the 2D ground state. The upper panel corresponds to a laser frequency in resonance with the plasmon, the middle panel to SHG into resonance and the lower panel to an arbitrary frequency unconnected to the plasmon. The laser intensity is $I = 10^{11}$ W cm^{-2} and polarisation is along z-axis in all cases.

3.2 Dependence on laser frequency

The dependence of SHG on the laser frequency is illustrated in Figure 2 in the case of the 2D ground state. We use here lasers polarised along z-axis in all presented cases and look at SHG for 3 frequencies. In the upper panel the laser frequency has been chosen in resonance with the plasmon along z-axis ($\omega_{\rm laser} = \omega_{\rm plasmon} = 3.6$ eV, Tab. 1), while in the middle panel the laser frequency has been chosen at half the plasmon frequency (so that the SHG signal is into resonance). Finally the lowest panel displays a case fully out of resonance ($\omega_{\rm laser} = 1.4$ eV). It is first interesting to note that this latter case exhibits the most fuzzy spectra. Because the laser frequency has no relation to the plasmon we only see a marked peak at the laser frequency

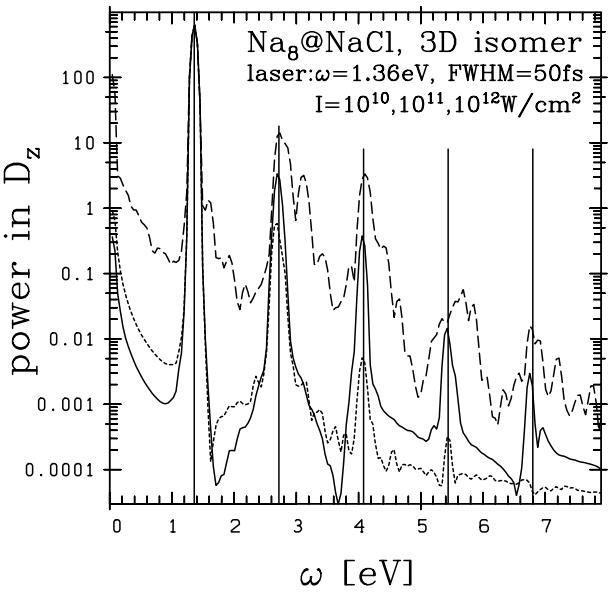

Fig. 3. Influence of laser intensity (as indicated in the figure) on SHG response in the case of the 3D isomer. Intensities are (in units of W/cm^2): dotted = 10^{10}, full = 10^{11}, dashed = 10^{12}. The laser is polarised along a z-direction perpendicular to the surface and the response is measured along the same direction.

and little beyond that. We are facing a typical off resonance behaviour in which there is virtually no response of the cluster of its own [28]. The two upper panels display more interesting cases in terms of SHG and exhibit very different behaviours. In the $\omega_{\rm laser} = 3.6$ eV case, the SHG signal is strongly reduced with respect to the direct signal (about a factor 20 000) which reflects the impact of the plasmon in enhancing the electronic response. The laser with frequency $\omega_{\rm laser} = 1.8$ eV, on the contrary exhibits an enhanced SHG (in resonance with the plasmon) with a much smaller reduction factor (only about a factor 100) and higher harmonics also very clearly appear, all with large signal over noise ratios. Note also that this latter case exhibits the most narrow peaks. Finally it is interesting to look at the electronic response along the principal axes of the cluster perpendicular to the laser polarisation (hence parallel to the surface). They are indicated on the three panels of Figure 2 by dashed and dashed-dotted lines and the respective power spectra have been normalized with respect to each other according to the amplitudes of the signals. In all cases, although one observes some cross talks, the response remains admittedly vanishingly small, perpendicularly to the laser polarisation.

3.3 Dependence on laser intensity

The impact of laser intensity on SHG is demonstrated for the example of the 3D isomer in Figure 3. We have considered here three typical laser intensities, as indicated on the figure. The laser polarisation has been chosen perpendicular to the surface (z-axis) in all cases and we show the dipole power also along this axis. The response along the other axes (parallel to the surface) is very small (a few %) and can be neglected here. As expected (see Sect. 2.3), the SHG signal strongly depends on the laser intensity, in particular in terms of the peak over noise ratio. We have normalized all direct response (*i.e.* at $\omega = \omega_{\rm laser}$) peaks to the same height. Thus we can read off that the ratio of SHG to the base harmonics grows proportional to I, as it should be. It is now very tempting to enhance the yield by arbitrarily increasing I. But the case with the highest intensity in Figure 3 shows already a sizeable spreading of the spectrum in the region of the second harmonics. This happens because the high intensity perturbs the system strongly, particularly by electron emission. Increasing the intensity one more order of magnitude destroys the spectrum completely. The optimum working point is then located at the largest intensity a safe bit below the intensity where the strong perturbation of the system becomes apparent and where the SHG signal is smeared out. For our case, we can deduce from Figure 3 that this point shows up at the intensity of $I = 10^{11}$ W/cm^2.

3.4 Dependence on laser polarisation

The last parameter to be varied is the laser polarisation which also plays an important role due to the highly anisotropic nature of our system. Excitation along the three principal axes is illustrated in Figure 4 for the case of the 2D ground state. Each figure corresponds to a different direction for polarisation. The SHG signal is recorded for each case along the axis in which the system had been excited. Again, cross talk is small in all cases and not further considered here. To establish comparable conditions, we take the "optimal" intensity $I = 10^{11}$ W/cm^2 and choose the laser frequency $\omega_{\rm laser}$ so that the second harmonics exactly matches the plasmon along the polarisation axis. This leads to choose $\omega_{\rm laser} = 1.77$ eV along z-axis, $\omega_{\rm laser} = 1.2$ eV along y-axis and $\omega_{\rm laser} = 0.85$ eV along x-axis, following the results of Table 1. Figure 4 shows that there is a marked difference between transverse (z-axis) and parallel (x- and y-axes) responses. The transverse SHG is extremely clean with high peak over background ratios and several visible higher harmonics. On the contrary, both parallel directions lead to more fuzzy responses. The second harmonic can be clearly identified in both cases but virtually no higher harmonic signal can be spotted, in particular along x-axis. This huge difference is related to the fact that the strongest symmetry breaking arises indeed in z-direction, orthogonal to the surface. Symmetry breaking parallel to the surface (*e.g.* by corrugation) does exist but is much smaller. The best condition for SHG is thus polarisation orthogonal to the surface which can practically be realised by arranging flat angle of the laser beam with respect to the substrate.

4 Conclusion

In this paper we have employed the time-dependent local-density approximation to investigate second harmonic

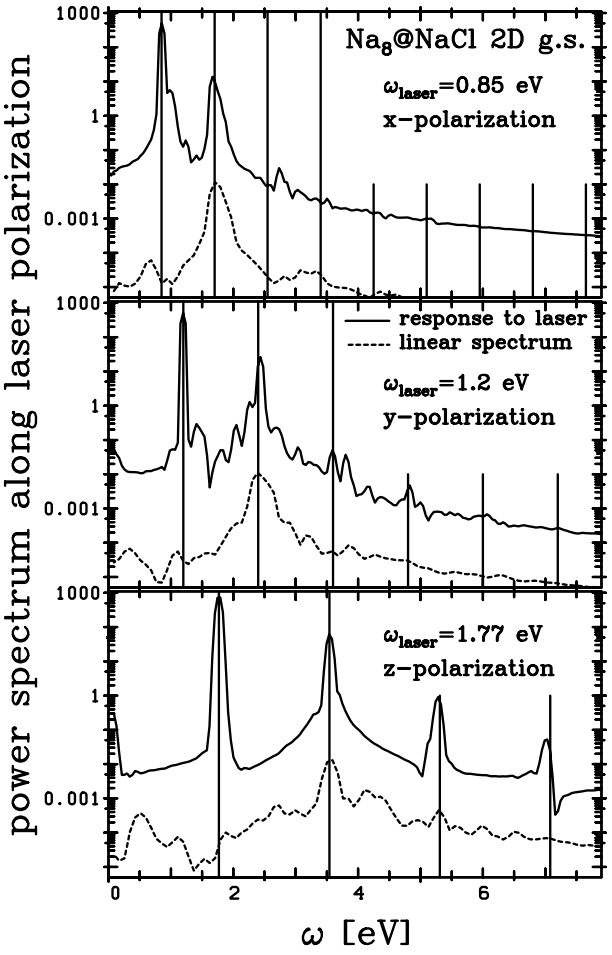

Fig. 4. Influence of laser polarisation on SHG response in the case of the 2D ground state. All laser irradiation have been performed with SHG "into resonance" (see text), and thus correspond to various laser frequencies for the different axes, as indicated on the figure. Dashed lines correspond to the linear response along the considered axis.

generation (SHG) in metal clusters deposited on an insulating substrate. The actual test case was Na_8 on NaCl. The attachment to a surface breaks reflection symmetry and thus enables SHG. This is precisely the situation in the experimental verification of SHG on clusters [16]. But our test case is, for technical reasons, much smaller than those actually used in these experiments. Nonetheless, our simple test system suffices for a first survey because the principle effects should be independent of system size.

We have successively considered the role of the various laser parameters. The pulse length was chosen very short (50 fs) to avoid interference with ionic motion during laser excitation and to simulate the experimental conditions where high intensity is related to short pulses. The frequency is most crucial. Optimal conditions are achieved if the double frequency coincides with the Mie plasmon resonance of the cluster. Good SHG are also obtained if one irradiates with the plasmon frequency. But this case produces relatively more electron emission and reaches earlier the limit of strong perturbations. Systematic variation of intensity I shows that the relative importance of the SHG signal grows with I^1. But the growth is limited very suddenly by a dissolution of the spectral signal because the too intense laser field destroys the system from which the second harmonics is to be generated. Concerning polarisation, it is the direction orthogonal to the surface which is most efficient in SHG. And that is obvious because this is the direction with the most pronounced symmetry breaking.

An open point remains the possible cross talk between the excitations along the three principal axes. We find that it is small but non-zero. This means that one has to deal, in principle, with a second order tensor for linear polarisability and a third order tensor for SHG giving rise to further interesting effects as, *e.g.*, optical activity. This needs yet to be explored in quantitative detail.

The authors thank the french-german exchange program PROCOPE number 99074 and Institut Universitaire de France for financial support during the realisation of this work.

References

1. W.A. de Heer, Rev. Mod. Phys. **65**, 611 (1993).
2. M. Brack, Rev. Mod. Phys. **65**, 677 (1993).
3. *Clusters of atoms and molecules*, edited by H. Haberland, Springer series in chemical physics **52** (Springer, Berlin, 1994).
4. *Metal clusters*, edited by W. Ekardt (Wiley, New-York, 1999).
5. F. Chandezon, C. Guet, B.A. Huber, D. Jalabert, M. Maurel, E. Monnand, C. Ristori, J.C. Rocco, Phys. Rev. Lett. **74**, 3784 (1995).
6. U. Näher, H. Göhlich, T. Lange, T.P. Martin, Phys. Rev. Lett. **68**, 3416 (1992); U. Näher, S. Frank, N. Malinowski, U. Zimmermann, T.P. Martin, Z. Phys. D **31**, 191 (1994).
7. U. Näher, S. Bjornholm, S. Frauendorf, F. Garcias, C. Guet, Phys. Rep. **285**, 245 (1997).
8. C. Bréchignac, Ph. Cahuzac, F. Carlier, M. de Frutos, Phys. Rev. Lett. **64**, 2893 (1990).
9. R. Schlipper, Ph.D. thesis, Freiburg, 1999
10. J.H. Klein-Wield, P. Simon, H.G. Rubahn, Phys. Rev. Lett. **80**, 45 (1998).
11. R.M. Dreizler, E.K.U. Gross, *Density Functional Theory: An Approach to the Quantum Many-Body Problem* (Springer-Verlag, Berlin, 1990)
12. A. Zangwill, P. Soven, Phys. Rev. A **21**, 1561 (1980).
13. F. Calvayrac, P.G. Reinhard, E. Suraud, J. Phys. B **31**, 5023 (1998).
14. K. Yabana, G.F. Bertsch, Phys. Rev. B **54**, 4484 (1996).
15. D. Östling, P. Stämpfli, K.H. Bennemann, Z. Phys. D **28**, 169 (1993).
16. M. Simon, F. Träger, A. Assion, B. Lang, S. Voll, G. Gerber, Chem. Phys. Lett. **296**, 579 (1998).
17. V.M. Akulin, E. Borsella, A.A. Nesterenko, Phys. Rev. Lett. **73**, 1231 (1994).
18. B. Montag, P.-G. Reinhard, Phys. Rev. B **51**, 14686 (1995).

19. C. Kohl, F. Calvayrac, P.-G. Reinhard, E. Suraud, Surf. Sci. **405**, 74 (1998).
20. H. Häkkinen, M. Manninen, Europhys. Lett. **34**, 177 (1996).
21. C. Kohl, P.-G. Reinhard, Z. Phys. D **39**, 605 (1997).
22. W. Kohn, L.J. Sham, Phys. Rev. **140**, 1133 (1965).
23. F. Calvayrac, P.-G. Reinhard, E. Suraud, J. Phys. B **31**, 1367 (1998).
24. O. Gunnarsson, B.I. Lundqvist, Phys. Rev. B **13**, 4274 (1976).
25. C. Fiolhais, J. Perdew, S.Q. Armster, M. MacLaren, M. Brajczewska, Phys. Rev. B **51**, 14001 (1995).
26. J.M. Eisenberg, W. Greiner, *Nuclear Theory* (Amsterdam, North Holland 1970), Vol. 2
27. F. Calvayrac, P.-G. Reinhard, E. Suraud, Ann. Phys. (NY) **255**, 125 (1997).
28. C. Ullrich, P.G. Reinhard, E. Suraud, J. Phys. B **30**, 5043 (1997).
29. P.-G. Reinhard, E. Suraud, Eur. Phys. J. D **3**, 175 (1998).
30. K.J. Song, D. Heskett, H.L. Dai, A. Liebsch, E.W. Plummer, Phys. Rev. Lett. **61**, 1380 (1988).
31. A. Liebsch, Phys. Rev. B **40**, 3421 (1989).
32. F. Calvayrac, A. Domps, P.-G. Reinhard, E. Suraud, C. Ullrich, Eur. Phys. J. D **4**, 207 (1998).